

RESEARCH

Open Access



Dynamic alteration of intrinsic properties of the cerebellar Purkinje cell during the motor memory consolidation

Dong Cheol Jang^{1,2,3}, Geehoon Chung³, Sun Kwang Kim^{3,4} and Sang Jeong Kim^{1*} 

Abstract

Intrinsic plasticity of the cerebellar Purkinje cell (PC) plays a critical role in motor memory consolidation. However, detailed changes in their intrinsic properties during memory consolidation are not well understood. Here, we report alterations in various properties involved in intrinsic excitability, such as the action potential (AP) threshold, AP width, afterhyperpolarization (AHP), and sag voltage, which are associated with the long-term depression of intrinsic excitability following the motor memory consolidation process. We analyzed data recorded from PCs before and 1, 4, and 24 h after cerebellum-dependent motor learning and found that these properties underwent dynamic changes during the consolidation process. We further analyzed data from PC-specific STIM1 knockout (STIM1^{PKO}) mice, which show memory consolidation deficits, and derived intrinsic properties showing distinct change patterns compared with those of wild-type littermates. The levels of memory retention in the STIM1^{PKO} mice were significantly different compared to wild-type mice between 1 and 4 h after training, and AP width, fast- and medium-AHP, and sag voltage showed different change patterns during this period. Our results provide information regarding alterations in intrinsic properties during a particular period that are critical for memory consolidation.

Keywords Eye movement learning, Vestibular ocular reflex, Consolidation, Purkinje cell, Intrinsic plasticity

Introduction

Intrinsic plasticity is a long-lasting modification of intrinsic excitability that has been reported in various brain regions [1–5]. Being accompanied by synaptic plasticity, intrinsic plasticity can be induced bidirectionally [4, 6–8]. Previous studies have focused on changes in firing frequency to evaluate the magnitude of intrinsic plasticity, as this is the most representative feature of changes in neuronal excitability [4, 7]. Hence, little is known about how intrinsic properties, except the firing frequency, change after intrinsic plasticity. Investigating intrinsic properties, such as action potential (AP) onset time, threshold, half-width, and other factors, is essential to gain a comprehensive understanding of the physiological role of intrinsic plasticity and its underlying mechanisms [7].

*Correspondence:

Sang Jeong Kim
sangjkim@snu.ac.kr

¹ Department of Physiology, Neuroscience Research Center, Wide River Institute of Immunology, Seoul National University College of Medicine, 103, Daehak-ro, Jongno-gu, Seoul 03087, Republic of Korea

² Department of Brain and Cognitive Science, College of Natural Science, Seoul National University, 1, Gwanak-ro, Gwanak-gu, Seoul 08826, Republic of Korea

³ Department of Physiology, College of Korean Medicine, Kyung Hee University, 26 Kyungheedae-ro, Dongdaemun-gu, Seoul 02447, Republic of Korea

⁴ Department of East-West Medicine, Graduate School, Kyung Hee University, 26 Kyungheedae-ro, Dongdaemun-gu, Seoul 02447, Republic of Korea



© The Author(s) 2023. **Open Access** This article is licensed under a Creative Commons Attribution 4.0 International License, which permits use, sharing, adaptation, distribution and reproduction in any medium or format, as long as you give appropriate credit to the original author(s) and the source, provide a link to the Creative Commons licence, and indicate if changes were made. The images or other third party material in this article are included in the article's Creative Commons licence, unless indicated otherwise in a credit line to the material. If material is not included in the article's Creative Commons licence and your intended use is not permitted by statutory regulation or exceeds the permitted use, you will need to obtain permission directly from the copyright holder. To view a copy of this licence, visit <http://creativecommons.org/licenses/by/4.0/>. The Creative Commons Public Domain Dedication waiver (<http://creativecommons.org/publicdomain/zero/1.0/>) applies to the data made available in this article, unless otherwise stated in a credit line to the data.

Memory consolidation stabilizes newly acquired information for long-term storage [9]. The cerebellum participates in various memory consolidation processes, including motor memory and fear conditioning memory [10–21]. Cerebellar memory consolidation processes involve the firing frequency of the cerebellar Purkinje cell (PC) [13–17], which is critically affected by changes in synaptic activity [10–12], protein synthesis [18], and intrinsic plasticity of PC [20]. In this study, we sought to identify the detailed changes involved in the intrinsic plasticity in the memory consolidation process. Although several studies have reported persistent alterations in intrinsic excitability during the consolidation period [22, 23], it remains unknown which changes in intrinsic properties accompany persistent alterations during this process.

To achieve this goal, we used data from our previous study, which used a transgenic mouse model of cerebellar memory deficits [20]. Previously, we reported that PC-specific deletion of stromal interaction molecule 1 (STIM1^{PKO}) in mice resulted in memory consolidation deficits after eye movement learning [19, 20]. Interestingly, these mice showed a deficit in intrinsic plasticity [19, 20] in both directions without affecting synaptic plasticity [19]. Considering these unique characteristics, we investigated the changes in intrinsic properties related to memory consolidation. In a previous study, we trained mice using a training protocol and successfully induced both synaptic and intrinsic long-term depression in the wild-type. In the case of the STIM1^{PKO}, synaptic but not intrinsic plasticity was induced as expected. We then collected various data related to changes in intrinsic excitability at 1, 4, and 24 h after training [20]. In the current study, we investigated the changes in intrinsic properties at each time point and inquired into the significant changes related to consolidation levels in wild-type littermates and STIM1^{PKO} mice. We found that PC intrinsic plasticity includes various changes in intrinsic properties that are continuously modulated during the memory consolidation process in normal mice. Although the intrinsic properties of STIM1^{PKO} changed after training, the alteration patterns differed from those of wild-type littermates. This suggests that different ion channels are involved in the changes in the intrinsic properties at each time point, and the resulting changes determine the level of memory retention.

Methods

Animal and behavior test

PC-specific STIM1 knockout mice line was generated by crossing PCP2-Cre line with a STIM1-floxed line as reported in our previous study [19]. For all experiments, 9 to 11-week-old male mice were used. All surgical and

behavior testing procedures were similar to our previous paper [19]. Eye movement training was applied by giving associative visuo-vestibular stimulation. The visual and vestibular stimulations were simultaneously rotated out-of-phase with $\pm 5^\circ$ amplitude. Gain, which indicates the amount of memory, was calculated as the ratio of the response amplitude to the stimulus amplitude. A custom-built LabView (National Instrument) tool was used to collect and analyze data.

Slice preparation and whole-cell recording

All procedures for slice preparation and whole-cell recording were similar to our previous paper [20]. Before sacrificing mice for the slice, the mice experienced eye movement training and waited for a particular time (1, 4 and 24 h). 300 μm of coronal cerebellar slices, which include bilateral flocculus, were obtained by cutting with a vibratome slicer (Leica, VT1200). The brain was cut in ice-cold NMDG cutting solution containing the following (in mM): 93 NMDG, 93 HCl, 2.5 KCl, 1.2 NaH_2PO_4 , 30 NaHCO_3 , 20 HEPES, 25 Glucose, 5 sodium ascorbate, 2 Thiourea, 3 Sodium pyruvate, 10 $\text{MgSO}_4 \cdot 7\text{H}_2\text{O}$, 0.5 $\text{CaCl}_2 \cdot 2\text{H}_2\text{O}$ (pH 7.3). Slices were transferred to a recovery chamber containing NMDG-cutting solution kept at 32 °C for 10 min and then incubated at room temperature for 1 h in standard artificial cerebrospinal fluid containing the following (in mM): 125 NaCl, 2.5 KCl, 1 MgCl_2 , 2 CaCl_2 , 1.25 NaH_2PO_4 , 26 NaHCO_3 , 10 glucose. All recordings from the flocculus were performed in the microzone where the floccular midline subregion is responsible for horizontal eye movement [24].

Brain slices were placed in a recording chamber on an Olympus microscope (BX50WI) stage and perfused with standard artificial cerebrospinal fluid. EPC9 amplifier with PatchMaster software (HEKA Elektronik) and a multiclamp 700B amplifier with pClamp 10 (Molecular Device) were used to amplify signals. Signals were collected with 20 kHz sampling frequency and filtered at 2 kHz. Inhibitory inputs were blocked by 100 μM picrotoxin (Sigma). Patch pipettes (3–4 M Ω) were pulled from borosilicate glass and filled with internal solution containing the following: 9 KCl, 10 KOH, 120 K-glucuronate, 3.48 MgCl_2 , 10 HEPES, 4 NaCl, 4 Na_2ATP , 0.4 Na_3GTP and 17.5 sucrose (pH 7.25). In our recordings, membrane potentials were not corrected for the liquid junction potential, calculated 15.8 mV. The bridge balance was compensated after the whole cell was made. We discarded the data if the holding current when the cell was held at -70 mV was lower than -500 pA or series resistance was changed by more than 20%. The excitability of the cerebellar Purkinje cells was measured by injecting +600 pA for 500 ms from -70 mV of baseline potential. The voltage sag and input resistance (R_{in}) was

measured by applying hyperpolarizing current injection from -100 pA to -500 pA with increments of -100 pA for 1 s. As an extension of our previous report on LTD-IE [4], all recordings were done at room temperature.

Data analysis and statistics

The action potential (AP) onset time was measured by calculating the time delay from the acquisition of the current injection to the first spike. The AP threshold was determined by measuring the membrane potential where its velocity entered the range of 30–60 mV/ms [25]. AP amplitude was calculated as a difference between the threshold and positive peak. The full width at half maximum (FWHM) of AP was measured by calculating the time duration at the half maximum voltage of AP. The medium afterhyperpolarization (mAHP) was calculated as the voltage difference between the negative peak after the spike train and -70 mV baseline. The fast afterhyperpolarization (fAHP) was measured by subtracting the negative peak of AP from the AP threshold. To calculate the instantaneous frequency, we measured the interspike interval (ISI) by subtracting the peak time of each AP and the inverted ISI value. The amount of voltage sag determined as difference between the lowest peak and steady-state voltage during the hyperpolarizing current injection, and the R_{in} was calculated from the steady-state voltage and injected hyperpolarizing current. All data were imported and analyzed by custom-built python analysis code.

All statistical analyses were performed using Graphpad Prism 9. Two sample t-test, One-way ANOVA with Fisher's LSD post-hoc test and the two-way ANOVA test were used. All graphs are shown as mean \pm SEM. The asterisks *, **, and *** indicate $p < 0.05$, $p < 0.01$, and $p < 0.001$, respectively. Detailed statistical methods and n for each experiment are written in the figure legends.

Results

PC intrinsic plasticity involves changes in the rheobase current, AP onset time, threshold, and amplitude

We first investigated changes in the firing frequency of PCs over time following a training session for cerebellar learning. As we previously reported [20], the firing frequency was lowest in the group at the 1 h time point. Firing frequency recorded at 4 and 24 h after training showed a significantly increased firing frequency compared to that at 1 h, indicating that the firing frequency recovered gradually to a baseline level (sham) within 24 h (Fig. 1A). We then investigated the changes in the rheobase current, AP onset, and AP threshold, which are closely related to the firing frequency. Consistent with firing frequency changes, the rheobase current and AP onset time increased significantly at 1 h after

training (Fig. 1B, sham vs. 1 h, $p = 0.026$; Fig. 1C, sham vs. 1 h, $p = 0.020$). The statistical significance of the AP onset time recovered by 4 h after training as the firing frequency (Fig. 1A, 1 h vs. 4 h, $p = 0.045$; Fig. 1E, 1 h vs. 4 h, $p = 0.008$), but the rheobase current remained significantly increased at this time point (Fig. 1C, sham vs. 4 h, $p = 0.029$). Remarkably, the AP threshold was not altered at the 1 and 4 h time points but was significantly reduced at the 24 h time point (Fig. 2A, sham vs. 24 h, $p = 0.046$, $F_{1,30} = 4.35$). We interpreted that the AP threshold reduced continuously from the early stage and reached statistical significance at the end of consolidation, that is, the 24 h time point (Fig. 2A). These results indicate that although firing frequency at the 24 h time point was comparable to that of sham controls (i.e., baseline level), properties related to intrinsic excitability did not return to sham control levels. Instead, a gradual decrease in the AP threshold over 24 h implied that PC intrinsic plasticity occurred for at least 24 h following the end of the training session, with compensation for changes in the AP threshold. AP amplitude was considerably reduced after training (Fig. 2B). At the 1 h time point, AP amplitude was significantly reduced (Fig. 2B, sham vs. 1 h, $p = 0.026$, $F_{1,23} = 5.63$) and reversed at 4 h after training (Fig. 2B, 1 h vs. 4 h, $p = 0.019$, $F_{1,23} = 6.32$). In the case of STIM1^{PKO}, there were no significant alterations in these properties (Fig. 2C, D), indicating that these alterations were not involved when the STIM1^{PKO} mice underwent training.

PC intrinsic plasticity involves changes in AP width with up- and downstroke speeds

Next, we analyzed changes in properties related to AP width, including full-width at half-maximum (FWHM), upstroke, and downstroke of the spikes. Rapid changes in FWHM were observed in wild-type mice (Fig. 3A), and these changes were based on the reduction in upstroke and downstroke speeds (Fig. 3B, C). The FWHM at the 1 h time point was significantly higher than that at baseline (sham vs. 1 h, $p = 0.001$, $F_{1,23} = 14.0$). Although there were no statistically significant differences, both up- and downstroke speeds decreased at the 1 h time point (Fig. 3B, sham vs. 1 h, $p = 0.117$, $F_{1,23} = 2.64$; Fig. 3C, sham vs. 1 h, $p = 0.104$, $F_{1,23} = 2.86$). At the 4 h time point, however, the trend reversed, with FWHM being significantly lower than that at baseline (sham vs. 4 h, $p = 0.041$, $F_{1,28} = 4.59$) and at the 1 h time point (1 h vs. 4 h, $p < 0.001$, $F_{1,23} = 17.3$). At this time point, there were significant increases in the up- and downstroke speeds (Fig. 3B, 1 h vs. 4 h, $p = 0.007$, $F_{1,23} = 8.83$; Fig. 3C, 1 h vs. 4 h, $p = 0.004$, $F_{1,23} = 10.6$). The FWHM at the 24 h time point was higher than at the 4 h time point (4 h vs. 24 h, $p = 0.034$, $F_{1,30} = 4.92$) and was not significantly different

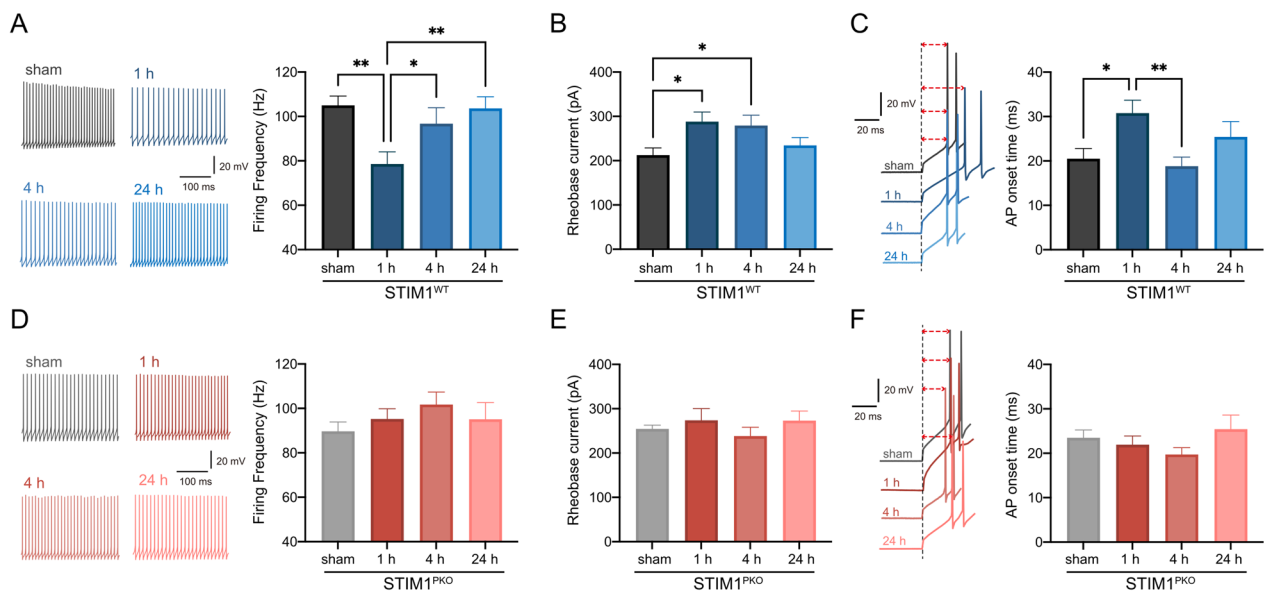


Fig. 1 LTD-IE includes firing frequency, rheobase current and AP onset time. **A** Firing frequency of wild-type through time. Firing frequency at the 1 h time point was significantly lower than all other time points ($F_{3,53} = 3.64$, $p = 0.018$; sham vs. 1 h, $p = 0.004$; 1 h vs. 4 h, $p = 0.045$; 1 h vs. 24 h, $p = 0.005$). **B** Rheobase current of wild-type through time. Rheobase currents at 1- and 4 h time points were significantly higher than sham control ($F_{3,53} = 3.13$, $p = 0.033$; sham vs. 1 h, $p = 0.017$; sham vs. 4 h, $p = 0.018$). **C** AP onset time of wild-type through time. AP onset time was significantly altered at the 1 h time point ($F_{3,53} = 3.12$, $p = 0.033$; sham vs. 1 h, $p = 0.020$; 1 h vs. 4 h, $p = 0.008$). **D** Firing frequency of $STIM1^{PKO}$ through time. There were no significant differences in firing frequency ($F_{3,53} = 1.31$, $p = 0.280$). **E** Rheobase current of $STIM1^{PKO}$ through time. The rheobase current was not significantly altered in $STIM1^{PKO}$ ($F_{3,53} = 0.737$, $p = 0.535$). **F** AP onset time of $STIM1^{PKO}$ through the time. There were no significant alterations ($F_{3,53} = 1.46$, $p = 0.237$). Sample numbers of wild-type (sham $n = 15$, 1 h $n = 10$, 4 h $n = 15$, 24 h $n = 17$) and $STIM1^{PKO}$ (sham $n = 16$, 1 h $n = 15$, 4 h $n = 16$, 24 h $n = 10$) are the same for all panels. One-way ANOVA with post hoc Fisher's LSD test was used for all panels. The graphs are shown as mean \pm SEM. * $p < 0.05$, ** $p < 0.01$

compared to the sham level. This alteration was based on the significant reduction in the downstroke speed at this time point (Fig. 3C, 4 h vs. 24 h, $p = 0.046$, $F_{1,30} = 4.32$). In contrast, $STIM1^{PKO}$ showed no alterations in these properties. FWHM was not significantly altered, although it slightly increased at the 1 h time point (Fig. 3D, sham vs. 1 h, $p = 0.250$, $F_{1,29} = 1.38$). Both up- and downstroke speeds did not change after training (Fig. 3E, F).

PC intrinsic plasticity accompanies different patterns of afterhyperpolarization, spike frequency adaptation, and sag voltage in wild-type and $STIM1^{PKO}$ mice

We then analyzed the changes in fast- and medium-afterhyperpolarization (AHP) and spike frequency adaptation (SFA) following training. Similar to the rapid changes in FWHM in wild-type mice (Fig. 3A), there was a significant elevation of fAHP at the 4 h time point (Fig. 4A, sham vs. 4 h, $p = 0.032$, $F_{1,28} = 5.12$; 1 h vs. 4 h, $p = 0.025$, $F_{1,23} = 5.72$; 4 h vs. 24 h, $p = 0.001$, $F_{1,30} = 13.1$). However, there was no alteration in mAHP levels in the wild-type (Fig. 4B, $p = 0.675$, $F_{3,54} = 0.513$). In contrast, $STIM1^{PKO}$ showed different patterns for these properties. There was a significant elevation of fAHP at the 1 h time point instead of the 4 h time point (Fig. 4C, sham

vs. 1 h, $p = 0.024$, $F_{1,29} = 5.68$), which was earlier than the wild-type. Interestingly, $STIM1^{PKO}$ showed an increase in mAHP at the 4 h time point, which was not observed in wild-type littermates (Fig. 4D, 1 h vs. 4 h, $p = 0.017$). The instantaneous frequency of wild-type mice decreased significantly at the 1 h time point (Fig. 4E, sham vs. 1 h, $p = 0.005$, $F_{1,23} = 9.40$) and returned to baseline levels at the 4 h time point. However, there was no change in the ISI ratio (Fig. 4F). Interestingly, $STIM1^{PKO}$ showed a significant increase in instantaneous frequency and ISI ratio at the 4 h time point (Fig. 4G and H). The alterations at the 4 h time point were significant at all other time points (Fig. 4G, sham vs. 4 h, $p = 0.012$, $F_{1,30} = 7.13$; 1 h vs. 4 h, $p = 0.047$, $F_{1,29} = 4.31$; 4 h vs. 24 h, $p = 0.047$, $F_{1,24} = 4.37$; Fig. 4H, sham vs. 4 h, $p = 0.006$; 1 h vs. 4 h, $p < 0.001$; 4 h vs. 24 h, $p = 0.002$). Next, we analyzed alterations in the R_{in} and sag voltage during negative current injection. In the wild-type, the R_{in} did not change at any time point (Fig. 5A). However, the sag voltage decreased significantly at the 1 h time point and was restored at the 4 h time point (Fig. 5B, sham vs. 1 h, $p = 0.043$, $F_{1,28} = 4.50$; 1 h vs. 4 h, $p = 0.048$, $F_{1,25} = 4.31$). $STIM1^{PKO}$ showed no significant alterations in either the R_{in} or sag voltage (Fig. 5C, D). Although there was a notable increase in R_{in}

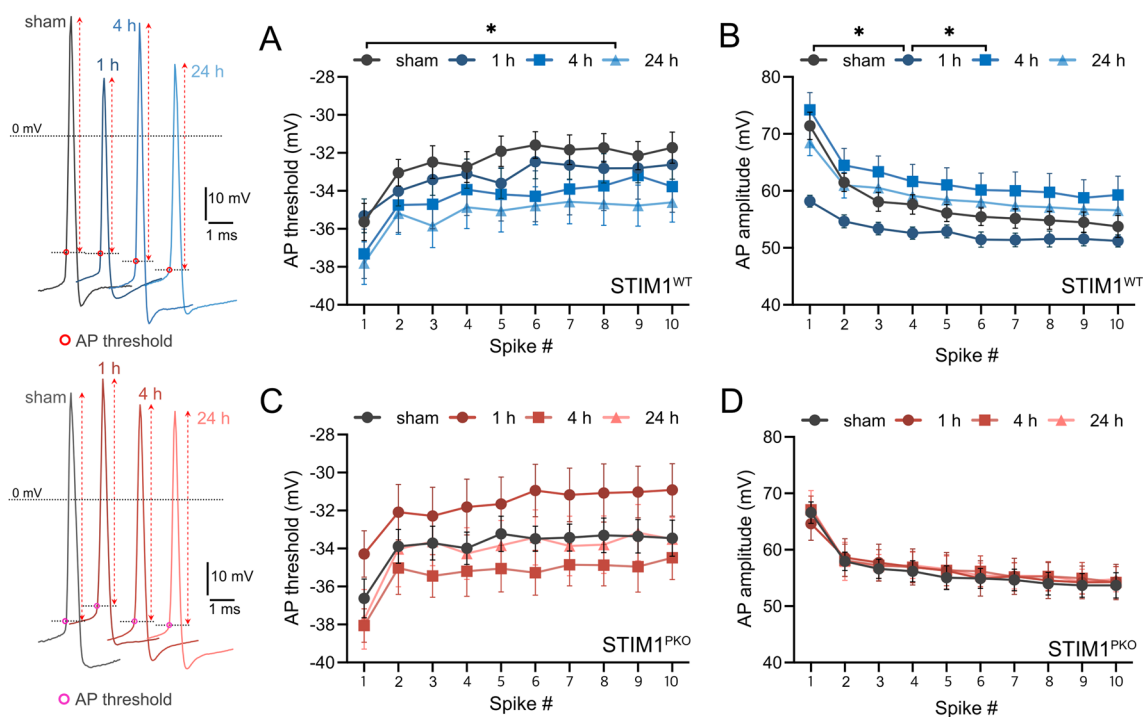


Fig. 2 LTD-IE affects the AP threshold and amplitude. In representative AP traces, AP thresholds are pointed by red (wild-type) or magenta circle (STIM1^{PKO}), and red arrows indicate AP amplitudes. **A** AP threshold of wild-type through time. AP threshold has been gradually decreased. It became significantly lower at the 24 h time point than the sham control ($F_{1,30}=4.35$, $p=0.046$). **B** AP amplitude of wild-type through time. AP amplitude was significantly altered at the 1 h time point compared to sham control and the 4 h time point (sham vs. 1 h, $F_{1,23}=5.63$, $p=0.026$; 1 h vs. 4 h, $F_{1,23}=6.32$, $p=0.019$). **C, D** AP thresholds and amplitudes were not significantly altered between the time points. Sample numbers of wild-type (sham $n=15$, 1 h $n=10$, 4 h $n=15$, 24 h $n=17$) and STIM1^{PKO} (sham $n=16$, 1 h $n=15$, 4 h $n=16$, 24 h $n=10$) are the same for all panels. Two-way ANOVA test was used for all panels. The graphs are shown as mean \pm SEM. * $p < 0.05$

at the 1 h time point, it was not statistically significant (Fig. 5C, sham vs. 1 h, $p=0.054$, $F_{1,26}=4.06$).

PC intrinsic properties of STIM1^{PKO} mice are comparable to wild-type

While wild-type mice showed time-dependent changes in firing frequency, rheobase, and AP onset time following training, STIM1^{PKO} mice showed no significant alterations compared to the baseline state (Fig. 1D–F). These results may be attributed to the occlusion of long-term depression of intrinsic excitability (LTD-IE) in STIM1^{PKO} mice, which is indicated by significantly lower levels of baseline firing frequency compared to wild-type mice [19]. As seen in the comparison between wild-type sham and post-training data (Figs. 2 and 3), intrinsic properties were significantly altered at the 1 or 4 h time points. We questioned whether plasticity deficiency in STIM1^{PKO} mice was accompanied by baseline alterations in intrinsic properties. To investigate this, we compared data from sham groups of wild-type and STIM1^{PKO} mice to determine whether there were any differences (Additional file 1: Fig. S1, Additional file 2: Fig. S2, Additional file 3: Fig. S3, Additional file 4: Fig. S4). As we reported,

the STIM1^{PKO} sham control showed a significantly lower firing frequency than the wild-type sham control (Figure S1A, $p=0.037$). No significant differences were found in the properties, including rheobase current, AP onset time (Additional file 1: Fig. S1B, C), AP threshold, AP amplitude, FWHM, up- and downstroke speeds (Additional file 1: Fig. S2), fAHP, mAHP (Additional file 1: Fig. S3A, B), and sag voltage (Additional file 1: Fig. S4B). The instantaneous frequency was slightly altered, but this change was not statistically significant (Additional file 1: Fig. S3C, $p=0.065$, $F_{1,30}=3.67$). The R_{in} decreased significantly for STIM1^{PKO} (Additional file 1: Fig. S4A, $p=0.016$, $F_{1,30}=6.55$), which is comparable to our previous results [19].

Discussion

Cerebellar learning includes two types of plasticity: synaptic and intrinsic [5]. In vestibular ocular reflex learning, synaptic LTD and LTD-IE are induced after gain-up training [20]. Deletion of STIM1 in Purkinje cells causes a deficit in intrinsic plasticity induction [19], and STIM1-deletion mice show severe memory deficiencies [19, 20]. These results imply that intrinsic plasticity directly

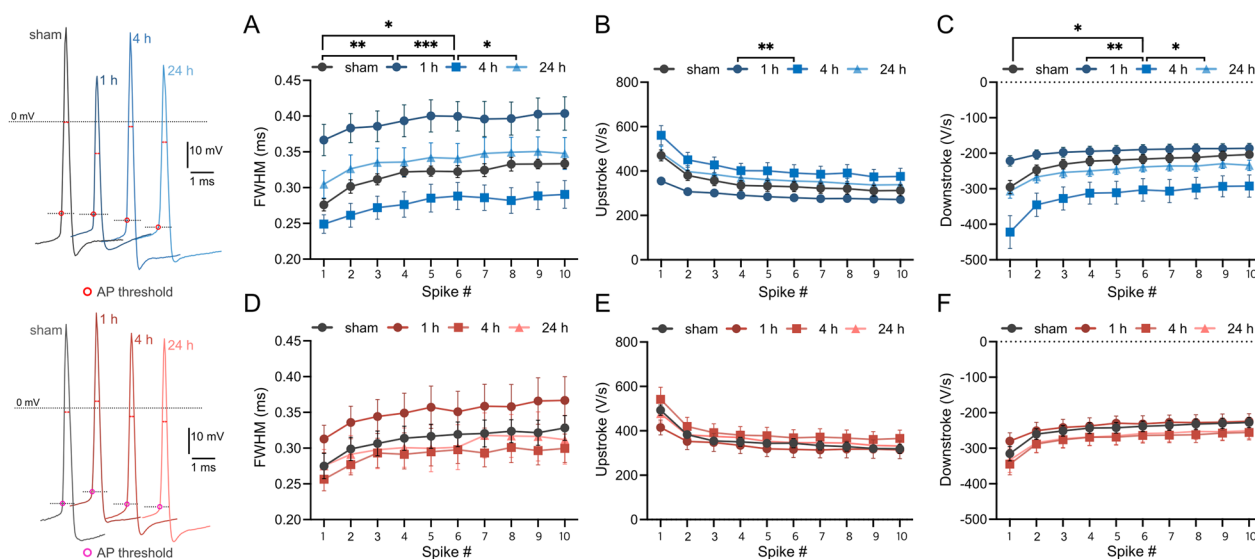


Fig. 3 LTD-IE affects AP shape differently between wild-type and $STIM1^{PKO}$. In representative AP traces, AP thresholds are pointed by red (wild-type) or magenta circle ($STIM1^{PKO}$), and red arrows indicate FWHM. **A** FWHM of wild-type through the time. FWHM was significantly increased at 1 h after training compared to sham control ($F_{1,23}=14.0, p=0.001$). The value of FWHM at the 4 h time point was significantly lower than all other time points (sham vs. 4 h, $F_{1,28}=4.59, p=0.041$; 1 h vs. 4 h, $F_{1,23}=17.3, p<0.001$; 4 h vs. 24 h, $F_{1,30}=4.92, p=0.034$). **B** Upstroke speed of wild-type through time. Upstroke speed was significantly increased between 1 and 4 h time points (1 h vs. 4 h, $F_{1,23}=8.49, p<0.008$). **C** Downstroke speed of wild-type through the time (sham vs. 4 h, $F_{1,28}=5.82, p=0.023$; 1 h vs. 4 h, $F_{1,23}=9.27, p=0.006$; 4 h vs. 24 h, $F_{1,30}=4.36, p=0.045$). **D–F** $STIM1^{PKO}$ showed no statistically significant alterations in FWHM, up- and down-stroke speeds. Sample numbers of wild-type (sham $n=15$, 1 h $n=10$, 4 h $n=15$, 24 h $n=17$) and $STIM1^{PKO}$ (sham $n=16$, 1 h $n=15$, 4 h $n=16$, 24 h $n=10$) are the same for all panels. Two-way ANOVA was used for all panels. The graphs are shown as mean \pm SEM. * $p<0.05$, ** $p<0.01$, *** $p<0.001$

contributes to memory consolidation. From this point of view, we compared the excitability of PCs between wild-type and $STIM1^{PKO}$. Comparing memory retention levels after eye movement learning from $STIM1^{PKO}$ with wild-type littermates, the differences became significant at the 4 h time point [20]. Because the retention levels of both groups were the same until 1 h after training, the time between 1 to 4 h after training, the intermediate stage, would be the critical period for the consolidation deficit in $STIM1^{PKO}$ mice. Intrinsic plasticity is thought to play a critical role in the intermediate stage of successful consolidation because no differences were observed in synaptic plasticity except intrinsic excitability until this stage [20]. In this study, wild-type and $STIM1^{PKO}$ mice showed different patterns of changes in intrinsic properties at this stage. While wild-type littermates showed an increase in AP up- and downstroke with a reduction in FWHM and an increase in fAHP and sag voltage, $STIM1^{PKO}$ showed a decrease in fAHP, and an increase in mAHP and SFA (Fig. 5). These results imply that changes in each genotype involve different channels, such as Na^+ , Ca^{2+} -activated K^+ (K_{Ca}), and hyperpolarization-activated cyclic nucleotide-gated (HCN) channels. We discuss the possible role of each channel in memory consolidation.

Voltage-gated Na^+ channels (Nav) contribute to AP amplitude and upstroke speed by generating Na^+ influx.

Partial blocking or reduced expression of voltage-gated Na^+ channels causes a notable decrease in AP amplitude and upstroke speed [26, 27]. Among the various types of voltage-gated Na^+ channels expressed in the cerebellum [28, 29], Nav1.6 (*Scn8a*) and Nav β 4 (*Scn4b*) play a critical role in PC neuronal excitability by contributing to the resurgent Na^+ current [30–32]. We observed a reduction in excitability with decreased AP amplitude and upstroke speed at the 1 h time point in wild-type mice, and these reduced properties were recovered during the intermediate stage (Figs. 1A, 2B, and 3B). These results imply that the resurgent Na^+ current might be reduced until 1 h after training and were then restored during the intermediate stage. In contrast, $STIM1^{PKO}$ mice showed no alterations in excitability, AP amplitude, or upstroke speed (Figs. 1D, 2D, and 3E). We previously reported the dysregulation of cytosolic Ca^{2+} concentration in $STIM1^{PKO}$ that leads to elevated intracellular Ca^{2+} concentrations [19]. Given that Ca^{2+} concentration is critically related to the permeability of Nav1.6 via CaMKII activity [33], persistently elevated intracellular Ca^{2+} concentrations in $STIM1^{PKO}$ mice may cause inflexible alterations in Nav1.6 permeability.

PCs express various K^+ channels, including voltage-gated K^+ and Ca^{2+} -activated K^+ channels (K_{Ca}) [29]. K^+ channels contribute to the repolarization of the AP by

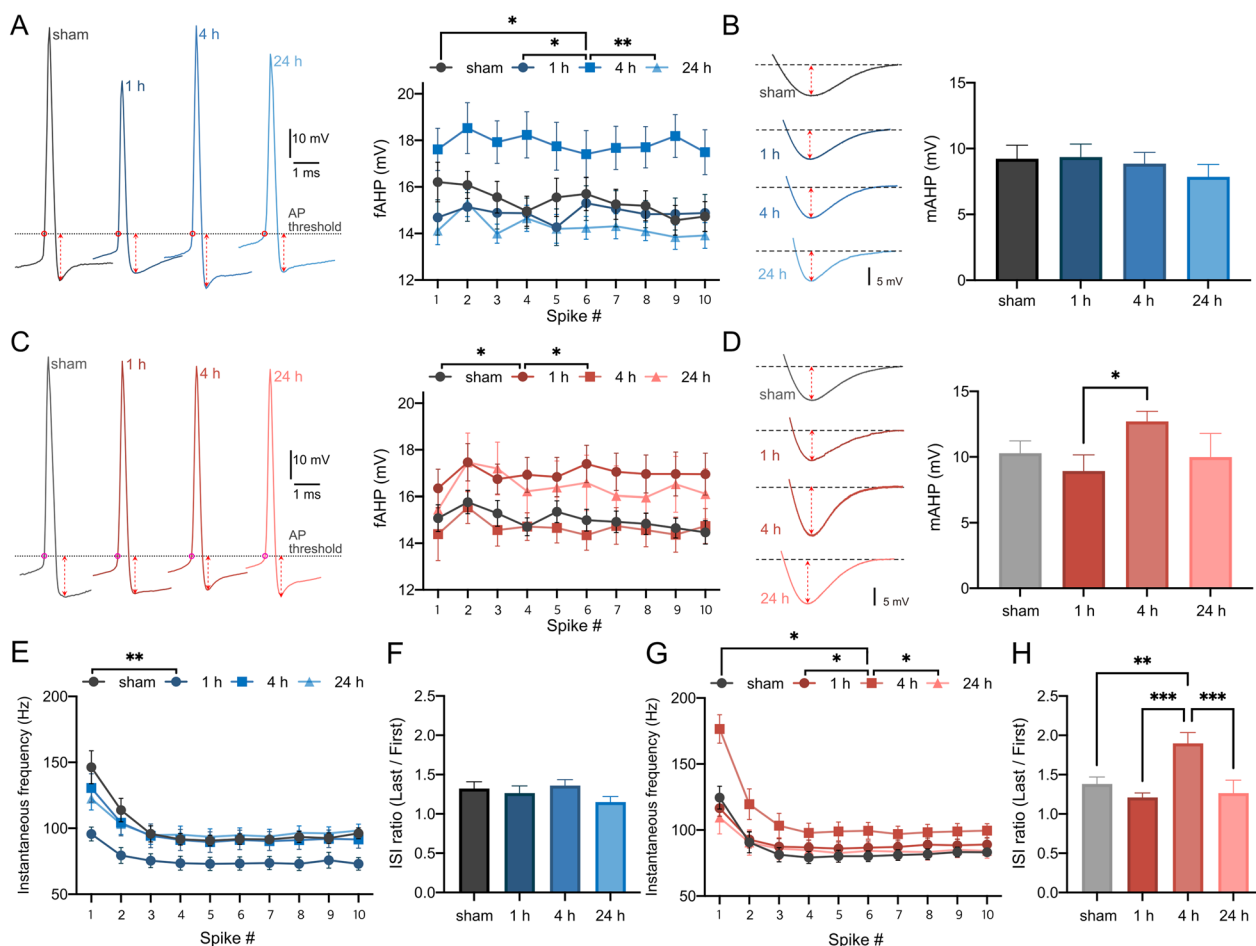


Fig. 4 Afterhyperpolarization and spike frequency adaptation of both genotypes after LTD-IE induction. **A** fAHP of wild-type through time points. Representative AP traces are aligned to its AP thresholds (red circle) for comparison. The value of fAHP at the 4 h time point was significantly lower than all other time points (sham vs. 4 h, $F_{1,28} = 5.12$, $p = 0.032$; 1 h vs. 4 h, $F_{1,23} = 5.72$, $p = 0.025$; 4 h vs. 24 h, $F_{1,30} = 13.1$, $p = 0.001$). **B** mAHP of wild-type through time points. There were no significant alterations between the time points ($F_{3,53} = 0.524$, $p = 0.667$). **C** fAHP of $STIM1^{PKO}$ through time points. Representative AP traces are aligned to its AP thresholds (magenta circles) for comparison. AP onset time was significantly altered at 1 h after training (sham vs. 1 h, $F_{1,29} = 5.68$, $p = 0.024$; 1 h vs. 4 h, $F_{1,29} = 5.52$, $p = 0.026$). **D** mAHP of $STIM1^{PKO}$ through time points. At the 4 h time point, mAHP was significantly increased than at the 1 h time point ($p = 0.017$). **E** The instantaneous frequency of wild-type through time. At the 1 h time point, the instantaneous frequency was significantly reduced compared to sham control (sham vs. 1 h, $F_{1,23} = 9.40$, $p = 0.005$). **F** ISI ratio of wild-type through time. There were no changes throughout the period ($F_{3,53} = 1.45$, $p = 0.239$). **G** The instantaneous frequency of $STIM1^{PKO}$ through time. At the 4 h time point, the instantaneous frequency was significantly higher in comparison to all other groups (sham vs. 4 h, $F_{1,30} = 7.14$, $p = 0.012$; 1 h vs. 4 h, $F_{1,29} = 4.32$, $p = 0.047$; 4 h vs. 24 h, $F_{1,24} = 4.38$, $p = 0.047$). **H** ISI ratio of $STIM1^{PKO}$ through time. Similar to instantaneous frequency, the value at the 4 h time point was significantly higher than other time points ($F_{3,53} = 8.22$, $p < 0.001$; sham vs. 4 h, $p = 0.001$; 1 h vs. 4 h, $p < 0.001$; 4 h vs. 24 h, $p < 0.001$). Sample numbers of wild-type (sham $n = 15$, 1 h $n = 10$, 4 h $n = 15$, 24 h $n = 17$) and $STIM1^{PKO}$ (sham $n = 16$, 1 h $n = 15$, 4 h $n = 16$, 24 h $n = 10$) are the same for all panels. Two-way ANOVA was used for **A**, **C**, **E** and **G**. One-way ANOVA with posthoc Fisher's LSD test was used for **B**, **D**, **F** and **H**. The graphs are shown as mean \pm SEM. * $p < 0.05$, ** $p < 0.01$, *** $p < 0.001$

generating a K^+ efflux. Blocking A-type voltage-gated K^+ channels increases the FWHM and decreases the downstroke speed in PCs [7], and D-type voltage-gated K^+ channels contribute to the intrinsic plasticity of hippocampal CA3 neurons [34]. Notably, we observed a significant reduction in FWHM and an increase in downstroke in wild-type mice during the intermediate stage, and these alterations recovered at the 24 h time point

(Fig. 3A, C). These results suggest that K^+ conductance significantly increased during the intermediate stage and recovered by 24 h after training. In addition to the reduction of FWHM, we observed an increased fAHP in wild-type mice at the 4 h time point (Fig. 4A), suggesting increased permeability of large-conductance Kca (BK channel) during the intermediate stage [35, 36]. The mAHP was not altered during the entire process

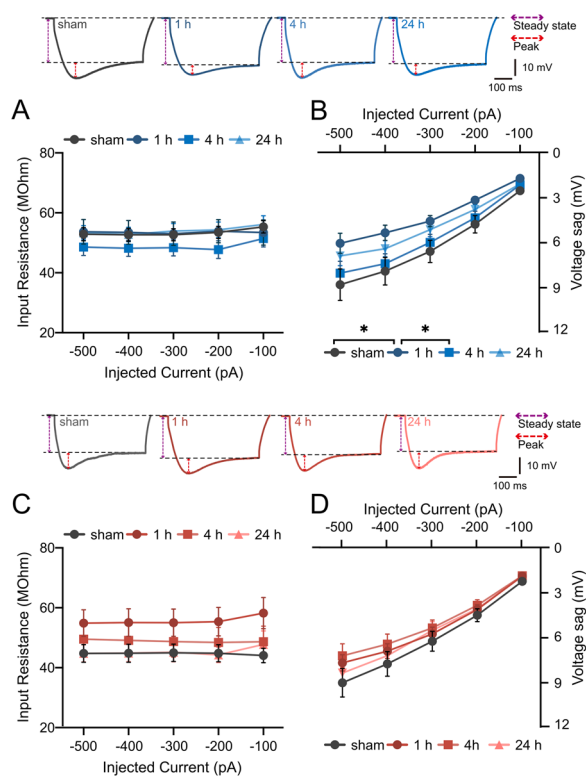


Fig. 5 Sag voltage was altered after LTD-IE induction. **A** R_{in} was not altered in wild-type. **B** Sag voltage at the 1 h time point was significantly lower than the sham and the 4 h time point (sham vs. 1 h, $F_{1,28}=4.50$, $p=0.043$; 1 h vs. 4 h, $F_{1,25}=4.31$, $p=0.048$). **C** R_{in} was not significantly altered in $STIM1^{PKO}$, although there was elevation at the 1 h time point (sham vs. 1 h, $F_{1,26}=4.06$, $p=0.054$). **D** There were no significant changes in sag voltage through time. Sample numbers of wild-type (sham $n=18$, 1 h $n=12$, 4 h $n=15$, 24 h $n=21$) and $STIM1^{PKO}$ (sham $n=14$, 1 h $n=14$, 4 h $n=14$, 24 h $n=9$) are the same for all panels. Two-way ANOVA was used for all panels. The graphs are shown as mean \pm SEM. * $p < 0.05$

(Fig. 4B). In contrast, $STIM1^{PKO}$ mice showed increased mAHP and SFA with no alteration in FWHM and downstroke speed at the 4 h time point (Figs. 3D, E, and 4D), implying increased permeability of small-conductance Kca (SK channel) during the intermediate stage [7, 37, 38]. The different activation of Kca observed in wild-type and $STIM1^{PKO}$ mice could potentially be attributed to the distinct distribution of SK and BK channels, leading to the utilization of distinct calcium sources [39, 40]. The distinct changes in the properties related to different K^+ channels suggest the critical involvement of PC firing fidelity in the memory consolidation process. With regard to memory consolidation in the cerebellum, the intermediate stage has been reported as a period for transferring newly acquired memory toward the deep cerebellar nucleus by plastic changes in PC firing [15, 18].

The alteration of BK channel permeability is involved in this process, as it is paranodally expressed in the axon, thereby contributing to modulation of the firing fidelity of PCs [41]. In contrast to the critical role of BK channel activity at the intermediate stage in the precise transfer of acquired information in the cerebellum, the deletion of SK channels in PCs did not lead crucial defects in eye movement learning and consolidation [42]. The deficits in memory consolidation in $STIM1^{PKO}$ mice may stem from insufficient fidelity of PC firing originating from altered K^+ channel permeability, although further studies are needed to clarify this.

The HCN channels are well-known contributors to hyperpolarization-activated current (Ih) channels [43] and are densely expressed in the cerebellum [44]. Previous studies have reported an essential role of this channel in the modulation of AP firing. For example, pharmacological blockade of HCN channels in GABAergic interneurons or GABAergic globus pallidus neurons reduces the firing frequency [45, 46]. HCN channels are known to affect neuronal excitability by modulating R_{in} [46, 47]. Our sag voltage results (Fig. 5B) indicate that HCN channel activity in wild-type mice was reduced within 1 h after training and was restored during the intermediate stage, which is similar to the time course of changes in firing frequency (Fig. 1A). Interestingly, there was no alteration in the R_{in} of the PCs (Fig. 5A), presumably because of compensation by other ion channels. We did not observe any alterations in sag voltage in $STIM1^{PKO}$ mice (Fig. 5D). As in the case of other channels, these results support the critical involvement of the Ca^{2+} concentration. HCN channel activity is affected by protein kinase C (PKC) activation [43, 47]. Because LTD-IE is also dependent on PKC signaling [4], disruption of the PKC pathway due to abnormal intracellular Ca^{2+} concentrations could cause abnormal intrinsic plasticity and HCN channel activity, leading to deficits in memory consolidation.

This study demonstrated dynamic alterations in intrinsic properties during eye movement memory consolidation (Fig. 6). We compared the alterations between wild-type and consolidation-deficient mice and inferred the possible contribution of various ion channels to the consolidation process. This study had some limitations. First, our analysis was based solely on the memory consolidation of eye movement behavior, although the cerebellum is involved in the learning of other characteristic behaviors, such as eye blink conditioning or fear conditioning [48–50]. Several studies have reported excitability changes in PCs after eye blink conditioning or fear conditioning [50, 51]. Investigating the intrinsic properties of PCs in other types of cerebellum-related

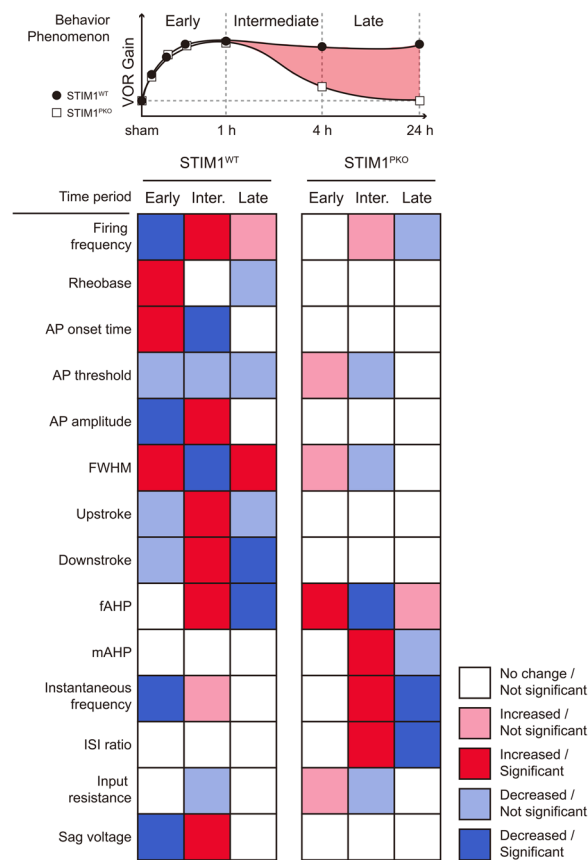


Fig. 6 Schematic summary of the study. In behavior, wild-type and STIM1^{PKO} mice showed similar gain values in the early stage (0 h to 1 h). However, the gain of STIM1^{PKO} mice significantly decreased during the intermediate stage (1 h to 4 h) and decreased more during the late stage (4 h to 24 h) (upper). In the intrinsic properties, wild-type mice showed dynamic and significant alterations in most of the properties, except mAHP and ISI ratio. However, most properties were not altered in STIM1^{PKO} mice, and even it seems that altered properties in STIM1^{PKO} mice are opposite to wild-type mice (below)

learning is expected to help elucidate the process of cerebellar memory consolidation. Secondly, our recordings were performed at room temperature to maintain the same recording conditions as in our previous study [4]. Because temperature is an influential factor for the opening probability of ion channels, the intrinsic properties may differ under physiological conditions. Finally, although STIM1^{PKO} showed a firm and clear phenotype, we only suggest a possible expectation in this study. Channel-specific modulation before, during, or after training is necessary to define the underlying mechanisms of the cerebellar memory process. Because these experiments are limited by several complications, computational modeling would be an acceptable approach.

Abbreviations

- PC Purkinje cell
- STIM1 Stromal interaction molecule 1
- STIM1^{PKO} Purkinje cell-specific STIM1 knockout
- LTD-IE Long-term depression of intrinsic excitability
- LTP-IE Long-term potentiation of intrinsic excitability
- AP Action potential
- FWHM Full-width half-maximum
- fAHP Fast afterhyperpolarization
- mAHP Medium afterhyperpolarization
- SFA Spike frequency adaptation
- R_{in} Input resistance
- Nav Voltage-gated Na⁺ channels
- ER Endoplasmic reticulum
- BK channel Large-conductance Ca²⁺-activated K⁺ channel
- SK channel Small-conductance Ca²⁺-activated K⁺ channel
- HCN channel Hyperpolarization-activated cyclic nucleotide-gated channel

Supplementary Information

The online version contains supplementary material available at <https://doi.org/10.1186/s13041-023-01043-9>.

Additional file 1: Fig S1. Comparison of firing frequency, rheobase current and AP onset time between sham groups of wild-type and STIM1^{PKO}. **A** STIM1^{PKO} showed reduced firing frequency than wild-type. **B, C** Rheobase current and AP onset times of both groups were not different. Sample numbers of wild-type and STIM1^{PKO} are the same for all panels. Two sample t-test was used for all panels. The graphs are shown as mean ± SEM. *p < 0.05.

Additional file 2: Fig S2. Comparison of AP shape with AP threshold between sham groups of wild-type and STIM1^{PKO}. In representative AP traces, AP thresholds are pointed by red magenta circle. There were no differences in **A** AP threshold, **B** AP amplitude, **C** FWHM, **D** Upstroke and **E** Downstroke. Sample numbers of wild-type and STIM1^{PKO} are the same for all panels. Two-way ANOVA was used for all panels. The graphs are shown as mean ± SEM.

Additional file 3: Fig S3. Comparison of afterhyperpolarization and spike frequency adaptation between sham groups of wild-type and STIM1^{PKO}. There were no significant differences in **A** fAHP, **B** mAHP, **C** Instantaneous frequency showed differences but could not fulfill statistical significance, **D** ISI ratio of both groups were on the same level. Sample numbers of wild-type and STIM1^{PKO} are the same for all panels. Two-way ANOVA was used for **A** and **C**. Two sample t-test was used for **B** and **D**. The graphs are shown as mean ± SEM. *p < 0.05, **p < 0.01.

Additional file 4: Fig S4. Comparison of R_{in} and sag voltage between sham groups of wild-type and STIM1^{PKO}. **A** The R_{in} of wild-type was significantly larger than STIM1^{PKO}. **B** There were no significant differences in the sag voltage. Sample numbers of wild-type and STIM1^{PKO} are the same for all panels. Two-way ANOVA was used for all panels. The graphs are shown as mean ± SEM. *p < 0.05

Acknowledgements

We thank Dr. HG Shim (Stanford University) and Dr. MS Bak (Neurogrin Inc.) for their valuable suggestions and comments.

Author contributions

DCJ conceptualized the study, analyzed the data and wrote the original and final manuscript. GC conceptualized the study and wrote the final manuscript. SKK and SJK supervised the study. All authors read and approved the final manuscript.

Funding

This research was supported by the National Research Foundation of Korea (NRF) grant funded by the Korean government (MSIT) (NRF-2021R1C1C1013840 to D.C.J.; NRF-2020R1C1C1009162 to G.C.; NRF-2019R1A2C2086052 to S.K.K.; NRF-2018R1A5A2025964 to S.J.K.).

Availability of data and materials

The datasets used and/or analyzed during the current study are available from the corresponding author upon reasonable request.

Declarations**Ethics approval and consent to participate**

All procedures were approved by the Institutional Animal Care and Use Committee of Seoul National University College of Medicine.

Consent for publication

Not applicable.

Competing interests

The authors have declared that no conflict of interest exists.

Received: 24 October 2022 Accepted: 10 June 2023

Published online: 10 July 2023

References

- Daoudal G, Debanne D. Long-term plasticity of intrinsic excitability: learning rules and mechanisms. *Learn Mem.* 2003;10:456–65. <https://doi.org/10.1101/lm.64103>.
- Zhang W, Linden DJ. The other side of the engram: experience-driven changes in neuronal intrinsic excitability. *Nat Rev Neurosci.* 2003;4:885–900.
- Mozzachiodi R, Byrne JH. More than synaptic plasticity: role of nonsynaptic plasticity in learning and memory. *Trends Neurosci.* 2010;33:17–26.
- Shim HG, Jang DC, Lee J, Chung G, Lee S, Kim YG, et al. Long-term depression of intrinsic excitability accompanied by synaptic depression in cerebellar purkinje cells. *J Neurosci.* 2017;37:5659–69. <https://doi.org/10.1523/JNEUROSCI.3464-16.2017>.
- Jang DC, Kim SJ. Plasticity leading to cerebellum-dependent learning: two different regions, two different types. *Pflügers Archiv Eur J Physiol.* 2019;471:927–34.
- Frick A, Magee J, Johnston D. LTP is accompanied by an enhanced local excitability of pyramidal neuron dendrites. *Nat Neurosci.* 2004;7:126–35.
- Belmeguenai A, Hossy E, Bengtsson F, Pedroarena CM, Piochon C, Teuling E, et al. Intrinsic plasticity complements long-term potentiation in parallel fiber input gain control in cerebellar Purkinje cells. *J Neurosci.* 2010;30:13630–43. <https://doi.org/10.1523/JNEUROSCI.3226-10.2010>.
- McElvain LE, Bagnall MW, Sakatos A, du Lac S. Bidirectional plasticity gated by hyperpolarization controls the gain of postsynaptic firing responses at central vestibular nerve synapses. *Neuron.* 2010;68:763–75.
- Dudai Y. The neurobiology of consolidations, or, how stable is the engram? *Annu Rev Psychol.* 2004;55:51–86.
- Boyden ES, Katoh A, Raymond JL. Cerebellum-dependent learning: the role of multiple plasticity mechanisms. *Annu Rev Neurosci.* 2004;27:581–609.
- Wulff P, Schonewille M, Renzi M, Viltono L, Sassoè-Pognetto M, Badura A, et al. Synaptic inhibition of Purkinje cells mediates consolidation of vestibulo-cerebellar motor learning. *Nat Neurosci.* 2009;12:1042–9.
- Galliano E, Gao Z, Schonewille M, Todorov B, Simons E, Pop AS, et al. Silencing the majority of cerebellar granule cells uncovers their essential role in motor learning and consolidation. *Cell Rep.* 2013;3:1239–51.
- Attwell PJE, Cooke SF, Yeo CH. Cerebellar function in consolidation of a motor memory. *Neuron.* 2002;34:1011–20.
- Cooke SF, Attwell PJ, Yeo CH. Temporal properties of cerebellar-dependent memory consolidation. *J Neurosci.* 2004;24:2934–41. <https://doi.org/10.1523/JNEUROSCI.5505-03.2004>.
- Kassardjian CD, Tan YFF, Chung JYJY, Heskin R, Peterson MJ, Broussard DM. The site of a motor memory shifts with consolidation. *J Neurosci.* 2005;25:7979–85. <https://doi.org/10.1523/JNEUROSCI.2215-05.2005>.
- Shutoh F, Ohki M, Kitazawa H, Itohara S, Nagao S. Memory trace of motor learning shifts transsynaptically from cerebellar cortex to nuclei for consolidation. *Neuroscience.* 2006;139:767–77.
- Okamoto T, Shirao T, Shutoh F, Suzuki T, Nagao S. Post-training cerebellar cortical activity plays an important role for consolidation of memory of cerebellum-dependent motor learning. *Neurosci Lett.* 2011;504:53–6.
- Okamoto T, Endo S, Shirao T, Nagao S. Role of cerebellar cortical protein synthesis in transfer of memory trace of cerebellum-dependent motor learning. *J Neurosci.* 2011;31:8958–66. <https://doi.org/10.1523/JNEUROSCI.1151-11.2011>.
- Ryu C, Jang DC, Jung D, Kim YG, Shim HG, Ryu H-H, et al. STIM1 regulates somatic Ca²⁺ signals and intrinsic firing properties of cerebellar Purkinje neurons. *J Neurosci.* 2017;37:8876–94. <https://doi.org/10.1523/JNEUROSCI.3973-16.2017>.
- Jang DC, Shim HG, Kim SJ. Intrinsic plasticity of cerebellar Purkinje cells contributes to motor memory consolidation. *J Neurosci.* 2020;40:4145–57.
- Sacchetti B, Baldi E, Lorenzini CA, Bucherelli C. Cerebellar role in fear-conditioning consolidation. *Proc Natl Acad Sci USA.* 2002;99:8406–11. <https://doi.org/10.1073/pnas.112660399>.
- Song C, Detert JA, Sehgal M, Moyer JR. Trace fear conditioning enhances synaptic and intrinsic plasticity in rat hippocampus. *J Neurophysiol.* 2012;107:3397–408.
- Chen L, Cummings KA, Mau W, Zaki Y, Dong Z, Rabinowitz S, et al. The role of intrinsic excitability in the evolution of memory: significance in memory allocation, consolidation, and updating. *Neurobiol Learn Mem.* 2020;173: 107266.
- Schonewille M, Luo C, Ruigrok TJH, Voogd J, Schmolesky MT, Rutteman M, et al. Zonal organization of the mouse flocculus: physiology, input, and output. *J Comp Neurol.* 2006;497:670–82. <https://doi.org/10.1002/cne.21036>.
- Kim C, Oh S, Lee JH, Chang SO, Kim J, Kim SJ. Lobule-specific membrane excitability of cerebellar Purkinje cells. *J Physiology.* 2012;590:273–88. <https://doi.org/10.1113/jphysiol.2011.221846>.
- Kalume F, Yu FH, Westenbroek RE, Scheuer T, Catterall WA. Reduced sodium current in purkinje neurons from Nav1.1 mutant mice: implications for ataxia in severe myoclonic epilepsy in infancy. *J Neurosci.* 2007;27:11065–74.
- Zhang J, Chen X, Eaton M, Wu J, Ma Z, Lai S, et al. Severe deficiency of the voltage-gated sodium channel Nav12 elevates neuronal excitability in adult mice. *Cell Rep.* 2021;36:109495.
- Schaller KL, Caldwell JH. Expression and distribution of voltage-gated sodium channels in the cerebellum. *Cerebellum.* 2003;2:2–9.
- Shim HG, Lee Y-S, Kim SJ. The emerging concept of intrinsic plasticity: activity-dependent modulation of intrinsic excitability in cerebellar purkinje cells and motor learning. *Exp Neurobiol.* 2018;27:139–54. <https://doi.org/10.5607/en.2018.27.3.139>.
- Raman IM, Bean BP. Resurgent sodium current and action potential formation in dissociated cerebellar purkinje neurons. *J Neurosci.* 1997;17:4517–26.
- Khalil ZM, Gouwens NW, Raman IM. The contribution of resurgent sodium current to high-frequency firing in purkinje neurons: an experimental and modeling study. *J Neurosci.* 2003;23:4899–912.
- Ransdell JL, Dranoff E, Lau B, Lo W-L, Donermeyer DL, Allen PM, et al. Loss of Navβ4-mediated regulation of sodium currents in adult Purkinje neurons disrupts firing and impairs motor coordination and balance. *Cell Rep.* 2017;19:532–44.
- Zyburas AS, Baucum AJ, Rush AM, Cummins TR, Hudmon A. CaMKII enhances voltage-gated sodium channel Nav1.6 activity and neuronal excitability. *J Biol Chem.* 2020;295:11845–65.
- Hyun JH, Eom K, Lee K, Ho W, Lee S. Activity-dependent downregulation of D-type K⁺ channel subunit Kv1.2 in rat hippocampal CA3 pyramidal neurons. *J Physiology.* 2013;591:5525–40.
- Womack MD, Khodakhah K. Characterization of large conductance Ca²⁺-activated K⁺ channels in cerebellar Purkinje neurons. *Eur J Neurosci.* 2002;16:1214–22.
- Kimm T, Khalil ZM, Bean BP. Differential regulation of action potential shape and burst-frequency firing by BK and Kv2 channels in substantia nigra dopaminergic neurons. *J Neurosci.* 2015;35:16404–17.
- Benda J, Herz AV. A universal model for spike-frequency adaptation. *Neural Comput.* 2003;15:2523–64.
- Gutkin B, Zeldenrust F. Spike frequency adaptation. *Scholarpedia.* 2014;9:30643.

39. Kaufmann WA, Ferraguti F, Fukazawa Y, Kasugai Y, Shigemoto R, Laake P, et al. Large-conductance calcium-activated potassium channels in purkinje cell plasma membranes are clustered at sites of hypolemmal microdomains. *J Comp Neurol*. 2009;515:215–30.
40. Blaustein MP, Golovina VA. Structural complexity and functional diversity of endoplasmic reticulum Ca²⁺ stores. *Trends Neurosci*. 2001;24:602–8.
41. Hirono M, Ogawa Y, Misono K, Zollinger DR, Trimmer JS, Rasband MN, et al. BK channels localize to the paranodal junction and regulate action potentials in myelinated axons of cerebellar Purkinje cells. *J Neurosci*. 2015;35:7082–94.
42. Grasselli G, Boele H-J, Titley HK, Bradford N, van Beers L, Jay L, et al. SK2 channels in cerebellar Purkinje cells contribute to excitability modulation in motor-learning-specific memory traces. *Plos Biol*. 2020;18: e3000596.
43. Brager DH, Johnston D. Plasticity of intrinsic excitability during long-term depression is mediated through mGluR-dependent changes in Ih in hippocampal CA1 pyramidal neurons. *J Neurosci*. 2007;27:13926–37.
44. Notomi T, Shigemoto R. Immunohistochemical localization of Ih channel subunits, HCN1–4, in the rat brain. *J Comp Neurol*. 2004;471:241–76.
45. Chan CS, Shigemoto R, Mercer JN, Surmeier DJ. HCN2 and HCN1 channels govern the regularity of autonomous pacemaking and synaptic resetting in globus pallidus neurons. *J Neurosci*. 2004;24:9921–32.
46. Roth FC, Hu H. An axon-specific expression of HCN channels catalyzes fast action potential signaling in GABAergic interneurons. *Nat Commun*. 2020;11:2248.
47. Shah MM. Cortical HCN channels: function, trafficking and plasticity. *J Physiology*. 2014;592:2711–9.
48. Sacchetti B, Scelfo B, Tempia F, Strata P. Long-term synaptic changes induced in the cerebellar cortex by fear conditioning. *Neuron*. 2004;42:973–82.
49. Zeeuw CID, Yeo CH. Time and tide in cerebellar memory formation. *Curr Opin Neurobiol*. 2005;15:667–74.
50. Titley HK, Watkins GV, Lin C, Weiss C, McCarthy M, Disterhoft JF, et al. Intrinsic excitability increase in cerebellar Purkinje cells after delay eye-blink conditioning in mice. *J Neurosci*. 2020;40:2038–46.
51. Zhu L, Scelfo B, Tempia F, Sacchetti B, Strata P. Membrane excitability and fear conditioning in cerebellar Purkinje cell. *Neuroscience*. 2006;140:801–10.

Publisher's Note

Springer Nature remains neutral with regard to jurisdictional claims in published maps and institutional affiliations.

Ready to submit your research? Choose BMC and benefit from:

- fast, convenient online submission
- thorough peer review by experienced researchers in your field
- rapid publication on acceptance
- support for research data, including large and complex data types
- gold Open Access which fosters wider collaboration and increased citations
- maximum visibility for your research: over 100M website views per year

At BMC, research is always in progress.

Learn more biomedcentral.com/submissions

